

12

Study of IEMP Effects on IC Operational Amplifier Circuits

ADA019667

M. J. BERNSTEIN and W. PASCHEN
Materials Science Laboratory
Laboratory Operations
The Aerospace Corporation
El Segundo, Calif. 90245

10 December 1975

Interim Report

APPROVED FOR PUBLIC RELEASE:
DISTRIBUTION UNLIMITED


DDC
RECEIVED
JAN 23 1976
RECEIVED

[Handwritten signature]

A

Prepared for
SPACE AND MISSILE SYSTEMS ORGANIZATION
AIR FORCE SYSTEMS COMMAND
Los Angeles Air Force Station
P.O. Box 92960, Worldway Postal Center
Los Angeles, Calif. 90009

Approved



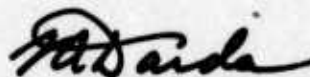
W. C. Riley, Director
Materials Sciences Laboratory
Laboratory Operations



E. L. Katz, Group Director
Development and Survivability
Directorate
Technology Division
Development Operations

This technical report has been reviewed and is approved for publication. Publication of this report does not constitute Air Force approval of the report's findings or conclusions. It is published only for the exchange and stimulation of ideas.

FOR THE COMMANDER



Larry A. Darda
Maj. United States Air Force
Program Manager
Survivability Directorate

UNCLASSIFIED

SECURITY CLASSIFICATION OF THIS PAGE (When Data Entered)

| REPORT DOCUMENTATION PAGE | | READ INSTRUCTIONS BEFORE COMPLETING FORM |
|--|-----------------------|--|
| 1. REPORT NUMBER 18 SAMSOTR-75-281 | 2. GOVT ACCESSION NO. | 3. RECIPIENT'S CATALOG NUMBER |
| 4. TITLE (and Subtitle) 6 STUDY OF IEMP EFFECTS ON IC OPERATIONAL AMPLIFIER CIRCUITS. | | 5. TYPE OF REPORT & PERIOD COVERED 9 Interim rept. |
| 7. AUTHOR(s) 10 Melvin J./Bernstein and Kenneth W./Paschen | | 8. CONTRACT OR GRANT NUMBER(s) 15 F04701-75-C-0076 |
| 9. PERFORMING ORGANIZATION NAME AND ADDRESS The Aerospace Corporation El Segundo, Calif. 90245 | | 10. PROGRAM ELEMENT, PROJECT, TASK AREA & WORK UNIT NUMBERS 12 30 P. |
| 11. CONTROLLING OFFICE NAME AND ADDRESS Space and Missile Systems Organization Air Force Systems Command Los Angeles, Calif. 90009 | | 12. REPORT DATE 11 10 December 1975 |
| 14. MONITORING AGENCY NAME & ADDRESS (if different from Controlling Office) | | 13. NUMBER OF PAGES 26 |
| | | 15. SECURITY CLASS. (of this report) Unclassified |
| | | 15a. DECLASSIFICATION/DOWNGRADING SCHEDULE |
| 16. DISTRIBUTION STATEMENT (of this Report) Approved for public release; distribution unlimited | | |
| 17. DISTRIBUTION STATEMENT (of the abstract entered in Block 20, if different from Report) | | |
| 18. SUPPLEMENTARY NOTES | | |
| 19. KEY WORDS (Continue on reverse side if necessary and identify by block number) IEMP Effects Operational Amplifier Radiation Effects TREE Responses X-Ray Responses | | |
| 20. ABSTRACT (Continue on reverse side if necessary and identify by block number) Three typical operational amplifiers were irradiated by a plasma focus to study their IEMP responses with and without superposition of TREE responses. The 30-kJ plasma focus device produced photons primarily in the 8- to 100-keV range with pulse widths typically in the range of 10 to 15 nsec. Pulses of electrons were also deposited on the external leads of the operational amplifiers to determine the characteristic responses. These units were operated in circuits with closed-loop gains ranging from 5 to 100. (cont on p 1473 B) | | |

DD FORM 1473 (FACSIMILE)

UNCLASSIFIED
SECURITY CLASSIFICATION OF THIS PAGE (When Data Entered)

009575

UNCLASSIFIED

SECURITY CLASSIFICATION OF THIS PAGE(When Data Entered)

19. KEY WORDS (Continued)

20. ABSTRACT (Continued) *fr p1473A*

During direct irradiation of the operational amplifiers, it was found that the IEMP responses (caused by photoemission within the housings) dominated the TREE responses provided that the RC time for the deposited charge to drain to ground was longer than a characteristic operational amplifier response time. The gas normally contained inside hermetically sealed operational amplifier units enhanced their IEMP responses. For most operational amplifiers, charge deposited on the input leads dominated the response, but some types were also sensitive to charge deposited on other external leads such as those controlling the offset.

1473B

A

| | |
|---------------------------------|---|
| ACCESSION for | |
| NTIS | White Section <input checked="" type="checkbox"/> |
| DDC | Gulf Section <input type="checkbox"/> |
| UNANNOUNCED | <input type="checkbox"/> |
| JUSTIFICATION..... | |
| BY..... | |
| DISTRIBUTION/AVAILABILITY CODES | |
| Dist. | AVAIL. and/or SPECIAL |
| <i>A</i> | |

UNCLASSIFIED

SECURITY CLASSIFICATION OF THIS PAGE(When Data Entered)

CONTENTS

| | | |
|------|---------------------------|----|
| I. | INTRODUCTION | 3 |
| II. | TEST CIRCUITS | 5 |
| III. | BENCH TESTS | 9 |
| IV. | IRRADIATION SETUP | 13 |
| V. | IRRADIATION RESULTS | 17 |
| VI. | DISCUSSION | 27 |

TABLE

| | | |
|----|--|---|
| I. | Parameters and Operating Specifications of Tested Operational Amplifiers | 6 |
|----|--|---|

FIGURES

| | | |
|----|--|----|
| 1. | Operational Amplifier Circuits Used During Testing | 7 |
| 2. | Output Signals from Q25 Operational Amplifier When Positive Charge Injected Alternately | 10 |
| 3. | Saturated Output Signals from Q25 Operational Amplifier with Charge Injected on Positive Input | 12 |
| 4. | Plasma Focus Irradiation Test Chamber and Configurations Used During Radiation Testing of Operational Amplifiers | 14 |
| 5. | Irradiation Responses of Q25 Operational Amplifier in ED Geometry for Different Environments | 18 |
| 6. | Responses of Q25 Operational Amplifier to Electron Deposition on External Heads with Collectors Attached | 20 |
| 7. | Radiation Responses of Two Sealed μ A702 Operational Amplifiers in Vacuum | 22 |
| 8. | Radiation Responses of Fairchild μ A702 Operational Amplifier for Different Environments with About the Same Irradiation | 23 |
| 9. | Radiation Responses of μ A741 Operational Amplifier Under Vacuum | 25 |

I. INTRODUCTION

As is well known, solid-state electronic circuits are very sensitive to photocurrents generated by transient penetrating radiation. Although effects that cause permanent damage are of greatest concern, serious problems also can arise when transient signals are generated. In particular, the outputs from analog circuits, such as those using operational amplifiers, can become saturated or distorted by extraneous current inputs. This study was aimed at understanding those signals caused by photoemission of electrons or Internal Electromagnetic Pulse (IEMP) effects inside and outside operational amplifier units and comparing them with those signals caused by deposition of photon energy in the transistor junctions or Transient Radiation Effects on Electronics (TREE) phenomena. In order to study such radiation effects on operational amplifiers, small circuits were exposed to pulsed photoelectron and x-ray environments generated by the Aerospace 30-kJ plasma focus device. The IEMP response studies were augmented by bench tests in which current was injected on the various external leads of operational amplifiers.

The mechanisms causing radiation-induced transient output signals from operational amplifiers can be classified conveniently into three groups: (1) photoemission and deposition of photoelectrons on the external leads of an operational amplifier, (2) photoemission within the operational amplifier housing, and (3) radiation interactions with the active solid-state junction regions (TREE). In the latter group, one might add the energy deposition from high-energy photoelectrons. The operational amplifiers and circuits selected for the test will first be described accompanied by the relevant results of the bench tests. Then, the setups for the plasma focus irradiation will be described, and the test results will be given and discussed.

II. TEST CIRCUITS

For the radiation testing of integrated circuit (IC) operational amplifiers, we used a model Q25AH unit made by Philbrick/Nexus Research (Teledyne) and models $\mu A702$ and $\mu A741$ made by Fairchild. This Q25 operational amplifier was a differential hybrid unit, with high-impedance FET inputs, that was made available to us for our first testing. The $\mu A702$ and $\mu A741$ units were readily available from inhouse stock. We chose the $\mu A702$ because of its simplicity (only nine transistors) and rather high speed, whereas the $\mu A741$ is a common, relatively slow unit with built-in frequency compensation. Bench tests were run on these three operational amplifiers as well as on a Fairchild $\mu A715$ and a Harris model HA-2620. As far as we could determine, all operational amplifiers were hermetically sealed with an atmosphere of dry N_2 within. Some of the Fairchild units had their housings opened so they could be evacuated or filled with gas. Relevant parameters and performance specifications of these operational amplifiers are listed in Table I. The Q25 had a grounded case, while all other types tested had the case connected to the negative supply.

These operational amplifier units were tested only as inverting and noninverting amplifiers with closed-loop gains of 2 up to 100. Input capacitances ranged from 3 to 6 pF. Typical circuits used are shown in Fig. 1. During radiation testing, the noninverting (positive) input was grounded through various values of resistance R_p , and the inverting (negative) input was grounded through various values of R_i . The feedback resistance R_f was normally much larger than the load resistance R_o . To avoid capacitive loading of the amplifier outputs by a long coaxial cable to an oscilloscope, a resistive load ranging from 500 to 5000 Ω was used in series with the terminated 50- Ω cable. Such voltage divisions resulted in signals at the oscilloscope that saturated around 50 mV to 1 V for the various models and values of load resistances.

Table 1. Parameters and Operating Specifications of Tested Operational Amplifiers

| Operational Amplifier Model No. | Nominal Input Resistance, Ω | Maximum Output Voltage, V | Frequency Response | | Open-Loop Gain, $\times 10^3$ | Built-In Frequency Compensation | Case Potential, V | Input Capacitance, pF |
|---------------------------------|------------------------------------|---------------------------|------------------------------|---------------------|-------------------------------|---------------------------------|-------------------|-----------------------|
| | | | Small-Signal Unity Gain, MHz | Maximum Output, kHz | | | | |
| Q25AH | $10^{12} \Omega$ | ± 9 | 30 | 100 | 2.0 | Yes | Ground | 6 |
| A702 | 32 k Ω | ± 4 | 10 | 100 | 3 | No | -6 | 3 |
| A741 | 2 M Ω | ± 10 | 1 | 10 | 200 | Yes | -15 | 5 |
| HA-2620 ^a | 100 M Ω | ± 10 | 100 | 500 | 100 | Yes | -15 | 4 |

^aThe HA-2620 unit was used only for a few bench tests.

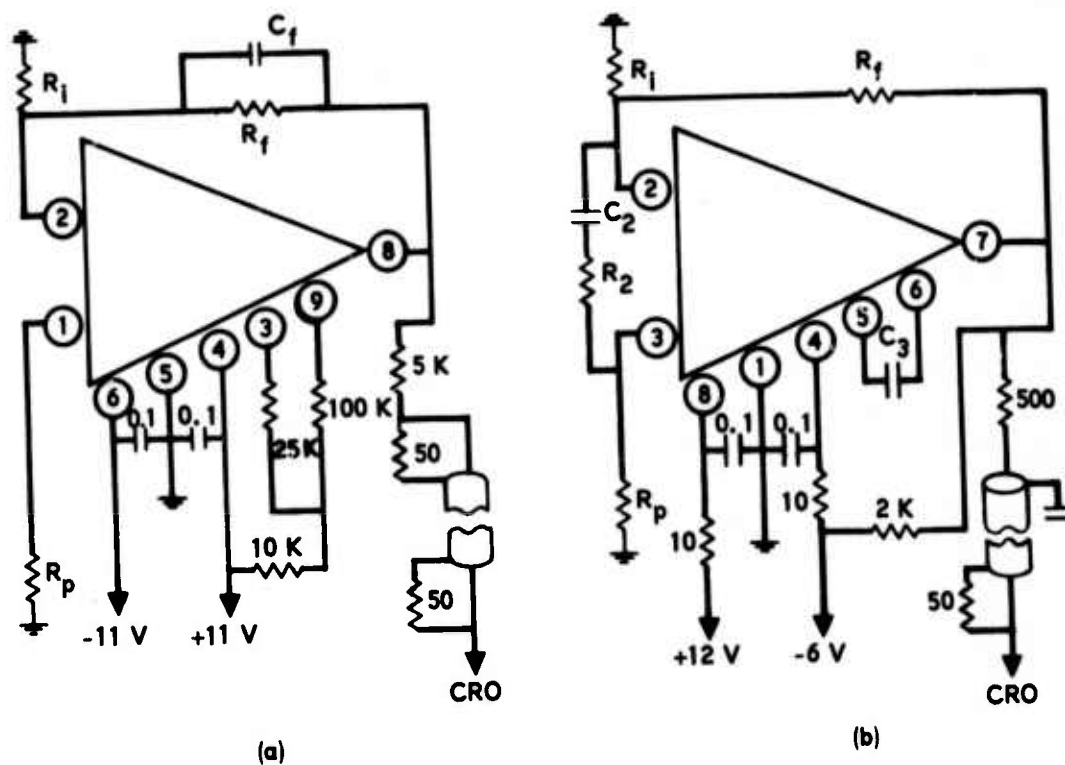


Fig. 1. Operational Amplifier Circuits Used During Testing: (a) Q25AH, and (b) μ A702. Circuit of μ A741 operational amplifier is similar, but with no frequency compensation.

III. BENCH TESTS

Different bench-test methods were used to inject pulsed currents on the external leads of an operational amplifier. The simplest method of applying a voltage pulse across a large resistance was not satisfactory, since large voltage transients were introduced. For most tests, electron deposition was simulated using the pulsed current from an RCA 931 photomultiplier tube (PM) operated in a grounded-anode configuration. Light pulses came from a light-emitting diode (LED) driven by a pulse generator; these light pulses had rise times of about 10 nsec and pulse widths of 20 to 150 nsec. We found the PM anode-to-ground capacitance to be about $C_{pm} = 9$ pF. Later, tests used the outputs from transistors to inject both positive and negative current pulses onto the leads; these units also had capacitances to ground of 9 ± 1 pF.

During much of the bench testing, the PM anode was connected directly to only one operational amplifier lead at a time; but some tests were done with current injected simultaneously on both inputs. The results of the bench tests can be divided into those where the amplifier output remained linear and those where it was driven into saturation. Consider first the signals resulting when positive current pulses were injected alternately or simultaneously on the Q25 inputs with $R_p = R_i = 50$ k Ω and $R_f = 500$ k Ω ($C_f = 10$ pF). The output signals are shown in Fig. 2. It is observed that the operational amplifier responds faster to charge placed on the positive input. Thus, when equal charge is placed on each of the two inputs, the positive input will dominate the output initially, and later in time, the output reverses from the predominantly positive pulse to a long-lasting, low-level negative signal.

When we increased the values of R_p relative to R_f , it was observed that the decay time of the amplifier output was dominated by the larger of the two values, $R_f C_f$ or $R_p C_p$. During tests on the Q25 with the parameters $R_i = R_f = 10$ k Ω with $C_f = 10$ pF, variations in R_p from 50 to 500 k Ω resulted in $1/e$ decay times of 0.7 to 7.5 μ sec in agreement with $C_p = 6$ pF and $C_{pm} = 9$ pF.

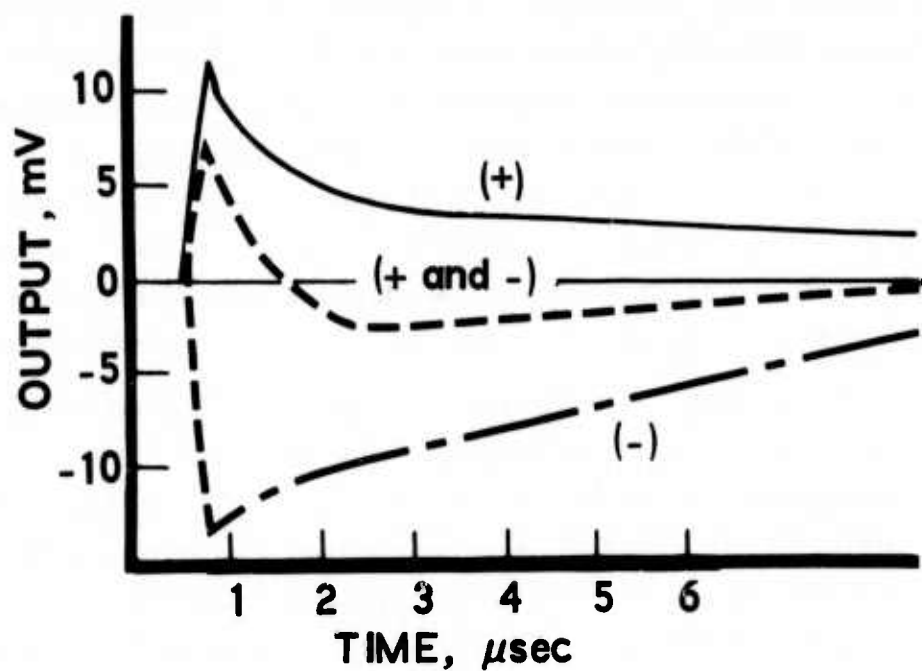


Fig. 2. Output Signals from Q25 Operational Amplifier When Positive Charge Injected Alternately on Positive Input Only (+), Negative Input Only (-), and Both Inputs Simultaneously (+ and -) for $R_p = R_i = 50 \text{ k}\Omega$ and $R_f = 500 \text{ k}\Omega$.

If larger values of capacitance were added to C_p , the RC decay time was increased with a corresponding decrease in the peak amplitude of the output signal.

The type and magnitudes of the output signals that result from injecting pulsed charge on each of the external leads of all the different operational amplifiers was studied. As might be expected, the magnitude of the output signals from charge deposited on the input leads depended on the values used for the input and feedback resistances. The responses of the Q25 and 702 units were relatively uncomplicated in that they were much more sensitive to charge deposited on the input leads than onto any of the other leads. Responses of the 741 and 2620 units were not so simple in that charge deposited on some of the leads used for compensation or for offset produced as large or even larger output signals than charge deposited on an input lead.

Now, consider the observations when enough charge was injected to drive an operational amplifier to saturation. We found an asymmetric behavior in the Q25, for instance, as shown in Fig. 3. When negative charge was injected on the positive input, the amplifier output saturated at the negative voltage, but at the end of saturation, the output rapidly dropped to the RC decay curve determined by a signal that did not saturate. For the injection of positive charge on the noninverting input of the Q25, the amplifier response depended on the $R_p C_p$ time constant and on the magnitude of the deposited charge. Consider the parameters $R_p = 100 \text{ k}\Omega$, $R_i = 100$, and $R_f = 10 \text{ k}\Omega$. The resulting outputs for increasing levels of injected charge are also shown in Fig. 3. For the largest input, the input first goes negative, then saturates for a while at the positive supply level, and then reverses to saturate at the negative supply level. When R_p was doubled in value or 10 pF placed across R_p , the operational amplifier output remained saturated at the positive level for a much longer time and did not reverse to end up in negative saturation.

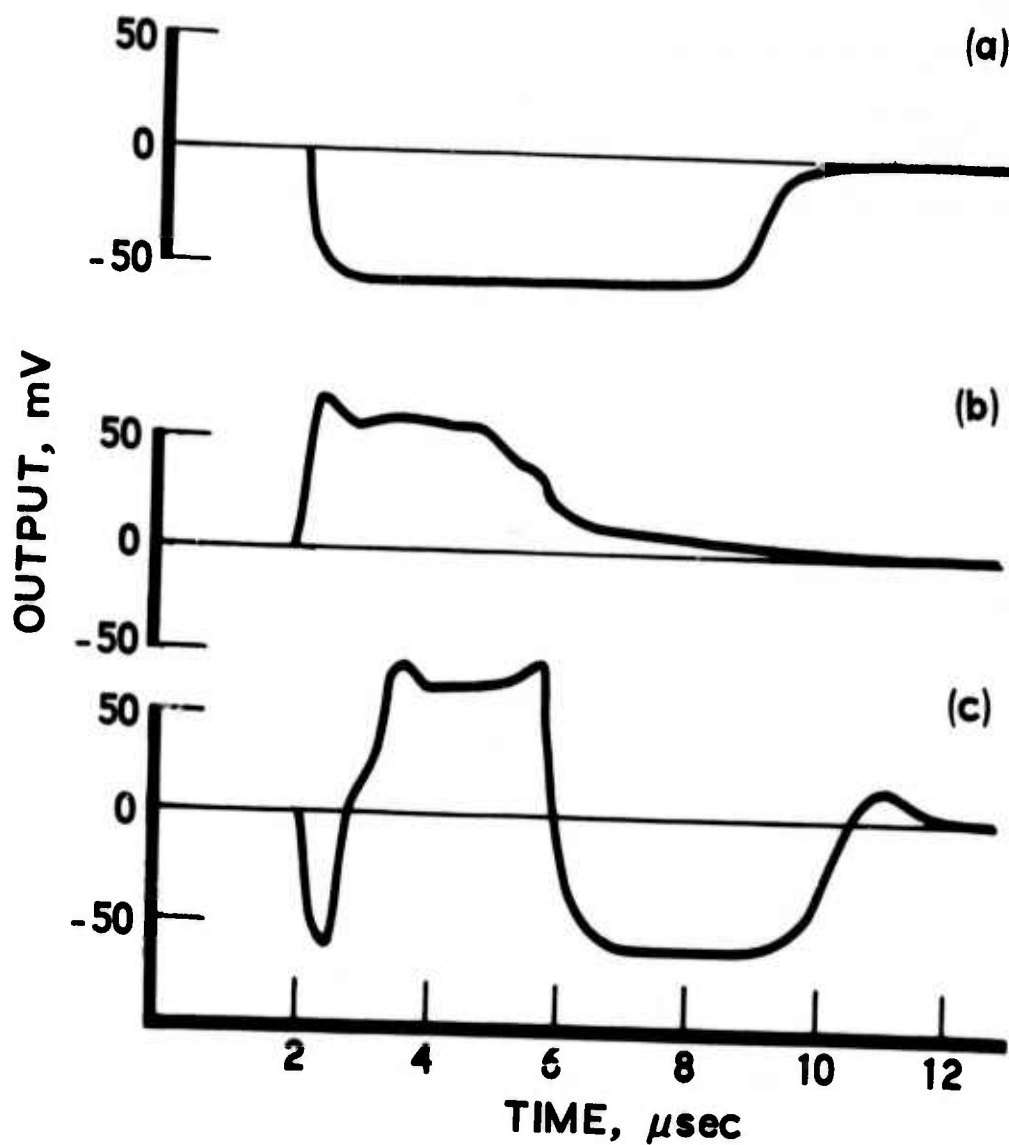


Fig. 3. Saturated Output Signals from Q25 Operational Amplifier with Charge Injected on Positive Input with $R_p = 100 \text{ k}\Omega$, $R_i = 100 \Omega$ and $R_f = 10 \text{ k}\Omega$: (a) Input of negative charge, (b) Input of positive charge, and (c) Increased input of positive charge.

IV. IRRADIATION SETUP

Pulsed x radiation was generated by the Aerospace 34-kJ Mark IV plasma focus device. An evacuable, electrically tight test chamber with an i.d. of 10.5 cm was mounted so that the emitted photons passed through a radiation window at the end of the chamber. Photon energies were primarily in the 8- to 100-keV range, and filters were normally used to transmit only photons above about 20 keV. Radiation pulse widths were 10 to 50 nsec, and dose rates generally ranged from 10^8 to 10^9 rad(Si)/sec. The integrated doses delivered through the operational amplifier covers ranged from 1 to 20 rad(Si). Characteristically, the x radiation from the plasma focus was somewhat harder on the more intense shots. This plasma focus and the test chamber have been used for previous pulsed irradiation studies.^{1,2}

Two types of configurations were used for the irradiation testing as shown in Fig. 4. One, shown in Fig. 4(a), was used primarily to study the effect of electron deposition (ED) on the Q25 operational amplifier circuit. The other, shown in Fig. 4(b), was employed for direct radiation (DR) testing on the operational amplifier circuits. For the ED tests, the circuit board was normally shielded from most of the direct radiation by 6 mm of Pb, while photoelectrons were emitted from thin Ta foils taped to an Al support placed in the radiation beam. This photoemission was greatly reduced in magnitude when the Ta foil was removed so that Al was the photoemitter. The electron flux incident on the circuit board was monitored by a small graphite sheet mounted adjacent to the circuit. In spite of the Pb shielding, some very hard radiation did penetrate or fluoresce off the Pb and interact with the amplifier.

¹M. J. Bernstein, "Radiation Induced Currents in Subminiature Coaxial Cables," IEEE Trans. Nucl. Sci. **NS-20**, 58 (1973).

²F. C. Tietze, A. E. Sanera, and R. H. Vandre, "A Minimal Photocurrent Analog Multiplexer Using Edge-On Diodes," IEEE Trans. Nucl. Sci. **NS-20**, 185 (1973).

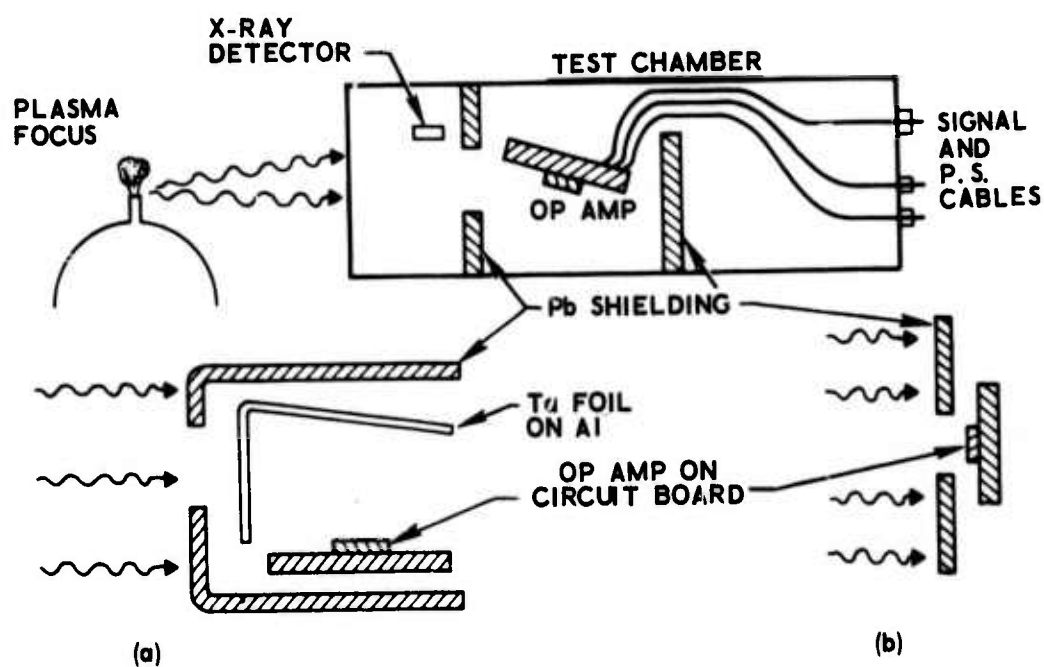


Fig. 4. Plasma Focus Irradiation Test Chamber and Configurations Used During Radiation Testing of Operational Amplifiers: (a) Electron deposition mode, and (b) Direct irradiation geometry.

Most irradiation data was taken with the test chamber evacuated to below 100 mTorr, but other shots were taken with the test chamber at atmospheric pressure. Since the Ta foils were about 6 cm from the circuit board, most photoelectrons were stopped by the air. When the radiation was unfiltered down to about 8 keV in energy, effectively, all the photoelectrons were stopped by the air. Some irradiation tests in the ED geometry were conducted with the Pb shield removed from in front of the circuit board. In this way, the relative magnitudes of signals caused by direct irradiation at oblique incidence could be compared with those caused by electron deposition on the circuit.

During DR tests in the geometry shown in Fig. 4(b), Pb was placed to shield various parts of the operational amplifier housing or the external circuitry. Advantages of the plasma focus as a radiation source are the predominance of photons below 70 keV and the small size of the source, which permits detailed shadowing of the radiation.³ Operational amplifiers other than the Q25 were tested in pairs to check equality of responses under the same irradiation or to compare their responses when one unit was shielded differently or evacuated.

³R. H. Vandre, "Effects of Shadows on Photocurrent Compensated Integrated Circuits," IEEE Trans. Nucl. Sci. NS-20, 180 (1973).

V. IRRADIATION RESULTS

During the early radiation testing, we concentrated on the effects of electron deposition under the external leads of the Q25 operational amplifier. A great deal of the data was taken using 100-nsec integrators on the signals from the operational amplifier, electron monitor, and x-ray detectors so that the quasiintegrated charge or dose could be more easily compared with the amplitude of the operational amplifier output. Tests on the Q25 were done with $C_f = 10$ pF; the circuit configurations could be classified as $R_p = 0$, $R_p = R_i$, and $R_p \gg R_i$.

For simplicity, consider first the results obtained with $R_p = 0$, $R_i = 50$ k Ω , and $R_f = 500$ k Ω ; five typical signals are shown in Fig. 5. The first four traces, obtained with the ED configuration shown in Fig. 4(a), were taken with and without air in the test chamber for the cases with and without Pb shielding in front of the circuit board. Removal of the Pb allowed the radiation to strike the operational amplifier at an oblique angle, while air in the chamber greatly reduced the number of photoelectrons reaching the circuit board from the Ta foil. The fifth trace was taken in the DR configuration with only low-z surfaces surrounding the circuit board. When Ta foil was placed to emit photoelectrons onto a circuit board, a short negative transient pulse appeared first on the amplifier output even with air present. For the shielded case, shown in Figs. 5(a) and (b), electron deposition on the negative input resulted in the broad positive output pulses that had 1/e decay times of $R_f C_f = 5.2 \pm 0.2$ μ sec; air in the chamber reduced the number of photoelectrons reaching the circuit. The broad, negative signals shown in Fig. 5(c) arose from an apparent cancellation of electron deposition on the external lead and photoemission from the same lead inside the operational amplifier. Observations similar to those shown in Figs. 5(a), (b), and (c) were obtained when circuit resistance values were reduced by a factor of 10. In this case, the observed 1/e decay time was now equal to $R_f C_f = 0.5$ μ sec.

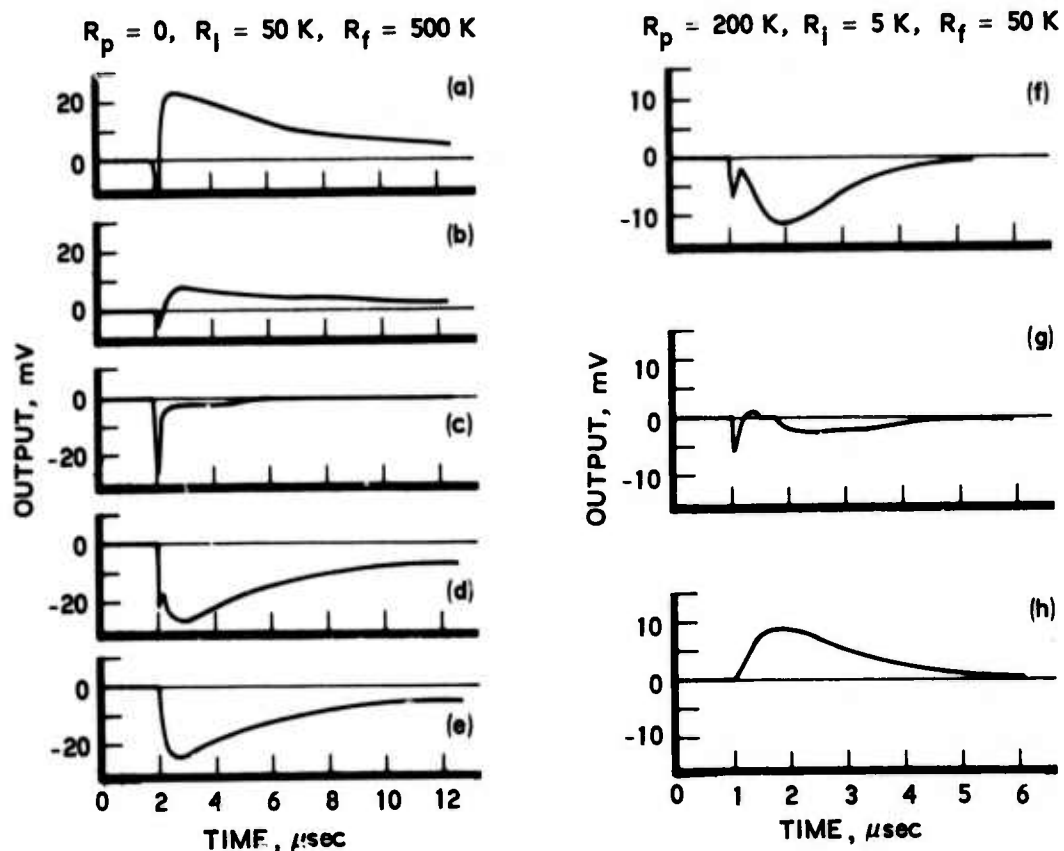


Fig. 5. Irradiation Responses of Q25 Operational Amplifier in ED Geometry for Different Environments: (a) Shielded unit in vacuum with Ta emitter, (b) Shielded unit in air with Ta emitter, (c) Shielded and open units in vacuum with Ta emitter, (d) Shielded and open units in air with Ta emitter, (e) Open unit in vacuum with Al emitter, (f) Open unit in vacuum with Ta emitter, (g) Open unit in air with Ta emitter, and (h) Shielded and open units in vacuum with Al emitter.

In general, for the shots represented by Fig. 5(a), there was a fairly linear relationship between the peak amplitudes of the initial negative output transient, positive output signal, electron-monitor signal, and x-ray signal. The largest deviation occurred for the most intense shot where the negative transient was extremely large and the broad positive amplitude relatively low. When the test chamber was filled with air, the positive output signal was reduced by a factor of 3 to 4, while the electron-collector signal decreased by a factor of 7 to 8. This can be explained by the larger average airpath from the photoemitter to the monitor than that to the circuit.

Other tests on the Q25 in the ED configuration were done with $R_p = 200 \text{ k}\Omega$, $R_i = 5 \text{ k}\Omega$, and $R_f = 50 \text{ k}\Omega$. Representative signals are also shown in Fig. 5(a). Again, a negative transient was observed arising from electron deposition on the output lead. Depending on whether the circuit was shielded or not, a broad negative or positive output signal was observed representing electron deposition or emission, respectively. The $1/e$ decay times of these broad signals corresponded to $R_p C_p = 1.3 \text{ }\mu\text{sec}$. When R_f was decreased to reduce the gain, the amplitude of the initial negative transient was greater than that of the broad negative pulse.

During the ED studies, we tried to reduce the effect of photoelectrons landing on the external leads. For simplicity, we used $R_p = 0$ on the Q25 and either placed a thick coating of low-z material on the negative lead or used a grounded low-z plate to shield the circuit from the photoelectrons. The signals on different shots were normalized to the electron deposition signal on the graphite monitor. It was found that the insulating coating reduced the amplifier output signal by about 30% while the grounded plate caused the broad signal to be decreased by a factor of 15.

Consider now the ED tests on the Q25 operational amplifier with the input resistances mostly in a so-called balanced condition where $R_p = R_f / (R_i + R_f)$. For $R_p = R_i = 1 \text{ k}\Omega$ and $R_f = 51 \text{ k}\Omega$, we get a signal such as shown in Fig. 6(a). Similar signals were observed if R_p and R_i were both increased

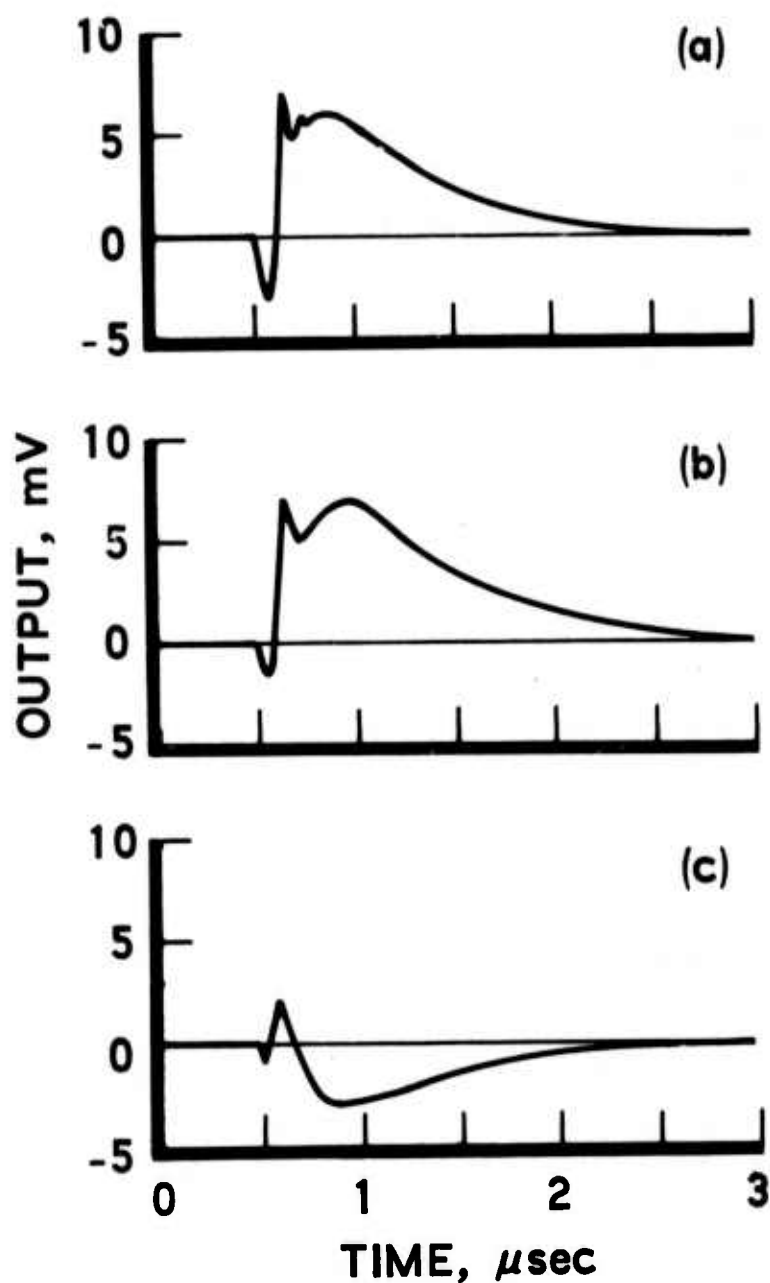


Fig. 6. Responses of Q25 Operational Amplifier to Electron Deposition on External Heads with Collectors Attached: (a) Typical of reproducible output with balanced input resistances, with $R_p = R_i = 1 \text{ k}\Omega$, and $R_f = 51 \text{ k}\Omega$; (b) and (c) Nonreproducible outputs from two consecutive shots with unbalanced input resistance, where $R_i = 5 \text{ k}\Omega$ and $R_p = R_f = 51 \text{ k}\Omega$.

to 5 k Ω . We then added small electron collectors with areas of 1 to 3 cm² to the inputs. To reduce the broad pulse very close to zero, the collector area on the positive input had to be about 50% larger than that on the negative input. But, there was still a rather large negative transient lasting about 150 to 200 nsec. It is interesting to compare what happens when the inputs were unbalanced with $R_p = R_f = 51$ k Ω and $R_i = 5$ k Ω . In this case, the output signals were not reproducible in form as evidenced by the signals from two consecutive shots shown in Figs. 6(b) and (c). The type of signal resulting from irradiation in this case did not correlate with x-ray intensity.

Let us now turn to the results from DR testing of the operational amplifiers. We start first with the simplest type tested, the Fairchild μ A702. Two units were irradiated side by side to compare responses under different conditions. It was found that identical exposure of two sealed units did result in the same responses. In order to determine what part of the radiation response arose from photons interacting with the IC chip, we shadowed one sealed unit with a small piece of Ta rod about 3 mm on a side (the operational amplifier housing was 6 mm in diam). Representative signals from the shadowed and unshadowed units on a typical shot are shown in Fig. 7. Note that the only difference is the absence of the initial large positive transient on the shadowed unit. In general, the μ A702 saturated at quite low dose levels. Next, it was of interest to find the effects of gas on the operational amplifier response. To do this, one of the units had a small hole cut in the corner of the Kovar lid. Typical signals resulting from comparable doses are shown in Fig. 8 for the following four cases: (a) sealed unit in vacuum, (b) open unit in N₂ atmosphere, (c) open unit in air, and (d) open unit in vacuum. It is seen that the largest responses occurred for the sealed and N₂-filled units. Other μ A702 samples were tested in the same way to ensure that these results were typical. When R_p was decreased to make a balanced configuration, the responses depended very much on the intensity of the radiation. On intense shots, the output exhibited first a large positive transient lasting about 100 nsec. Then, the signal went into negative saturation for a

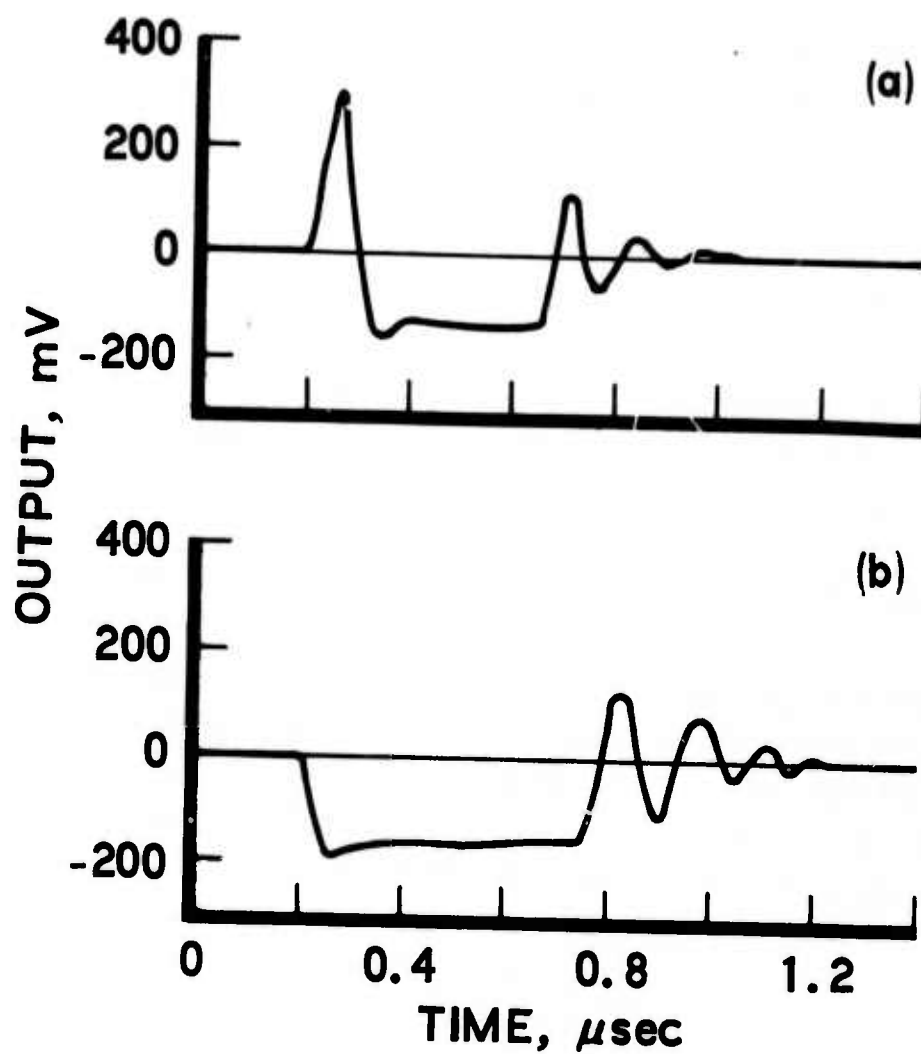


Fig. 7. Radiation Responses of Two Sealed μ A702 Operational Amplifiers in Vacuum: (a) Total exposure, and (b) IC chip shielded. Both samples exposed simultaneously where IC chip of one (b) was shielded from radiation by small Ta cylinder.

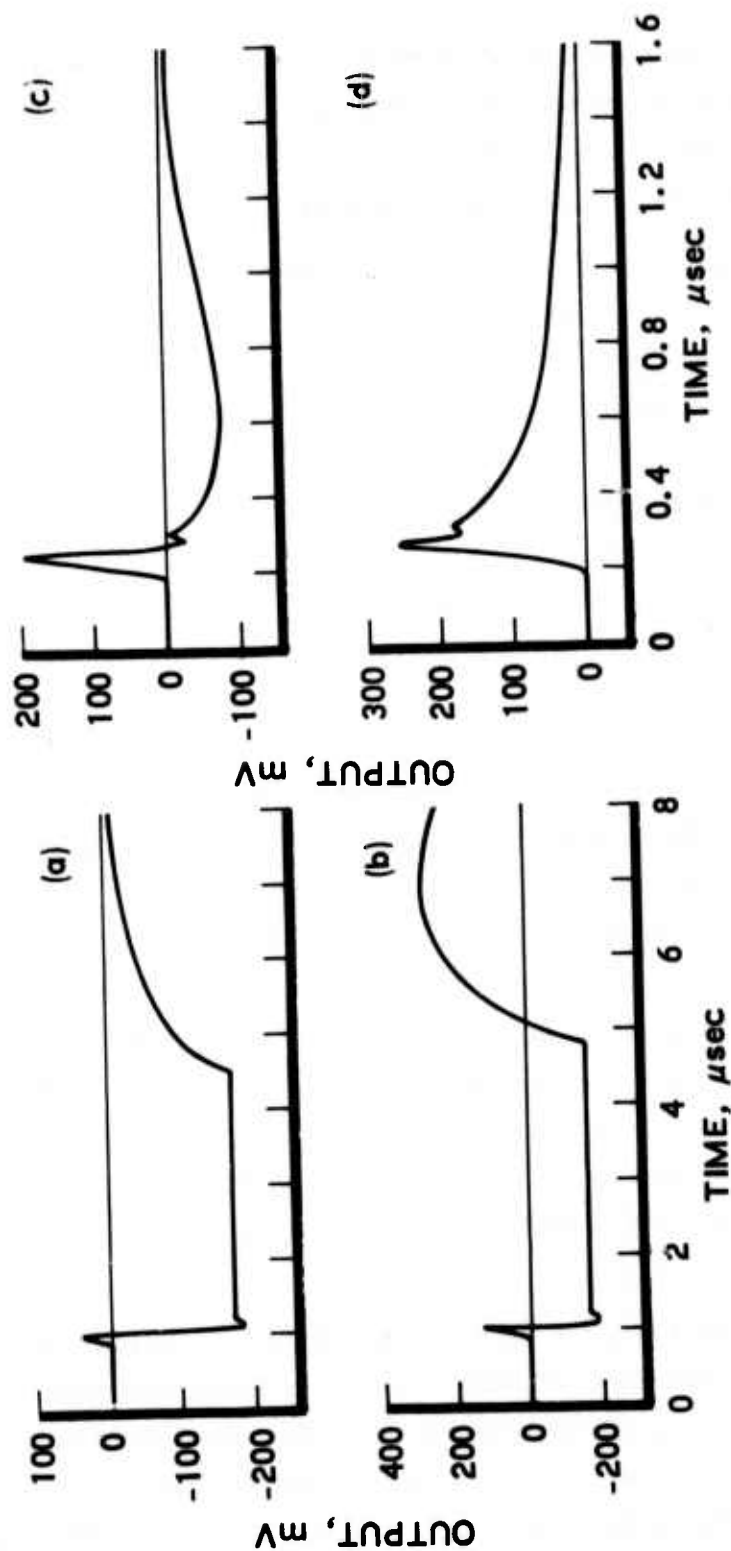


Fig. 8. Radiation Responses of Fairchild $\mu A702$ Operational Amplifier for Different Environments with About the Same Irradiation: (a) Sealed unit in vacuum, (b) Open unit in N_2 (response of sealed units in N_2 also shows late positive overshoot that is attributed to deposition of positive ions), (c) Open unit in air, and (d) Open unit in vacuum. Note different time scales.

sealed unit while it oscillated around zero for a unit that was evacuated or filled with air. On weaker shots, there were some initial oscillations around zero, and then the output went into negative saturation in a sealed unit, but went only slightly negative for an evacuated unit.

Radiation responses of Fairchild μ A741 units are examined next. The most important observation was that TREE dominated the IEMP effects in a μ A741. In other words, irradiation of the entire operational amplifier housing resulted in the same output signal regardless of whether the unit was sealed, evacuated, or filled with air. IEMP effects could be detected only when the IC chip was shadowed from the x rays by a small piece of Ta rod. Typical output signals from a μ A741 are shown in Fig. 9 for total exposure and shadowed exposures. For the totally exposed condition, Fig. 9(a), it is seen that a dominant positive signal follows an initial narrow negative transient. A nonsaturating signal was obtained only when the dose was quite low, and then the positive signal decayed with a time constant of about 16 μ sec. When the IC chip of a sealed unit was shadowed, Fig. 9(b), the output signal appeared to consist of the small initial negative transient followed by a superposition of positive signal and slower negative signal. The relative magnitudes of the positive and negative parts of the signal depended very much on the dose as shown in Fig. 9(a). It may be that some of the harder radiation associated with a more intense discharge was scattered and absorbed by the IC chip. When an open unit was irradiated under vacuum, Fig. 9(c), the slow negative component of the output signal was greatly reduced compared to that from a sealed unit. Various tests run in air or N_2 were greatly complicated by gas ionization in the vicinity of the external leads, particularly on the μ A741 type.

Finally, the DR tests on the Q25 are presented. Initial tests utilized $R_p = 0$ with $R_i = 50\text{ K}\Omega$ and $R_f = 500\text{ K}\Omega$. For these parameters, the whole circuit was irradiated, and Pb was placed to shadow the entire operational amplifier itself from the x rays or to shadow various leads to the operational amplifier. The important result here was that the signal caused by photoemission off the negative input inside the housing was about six times as large

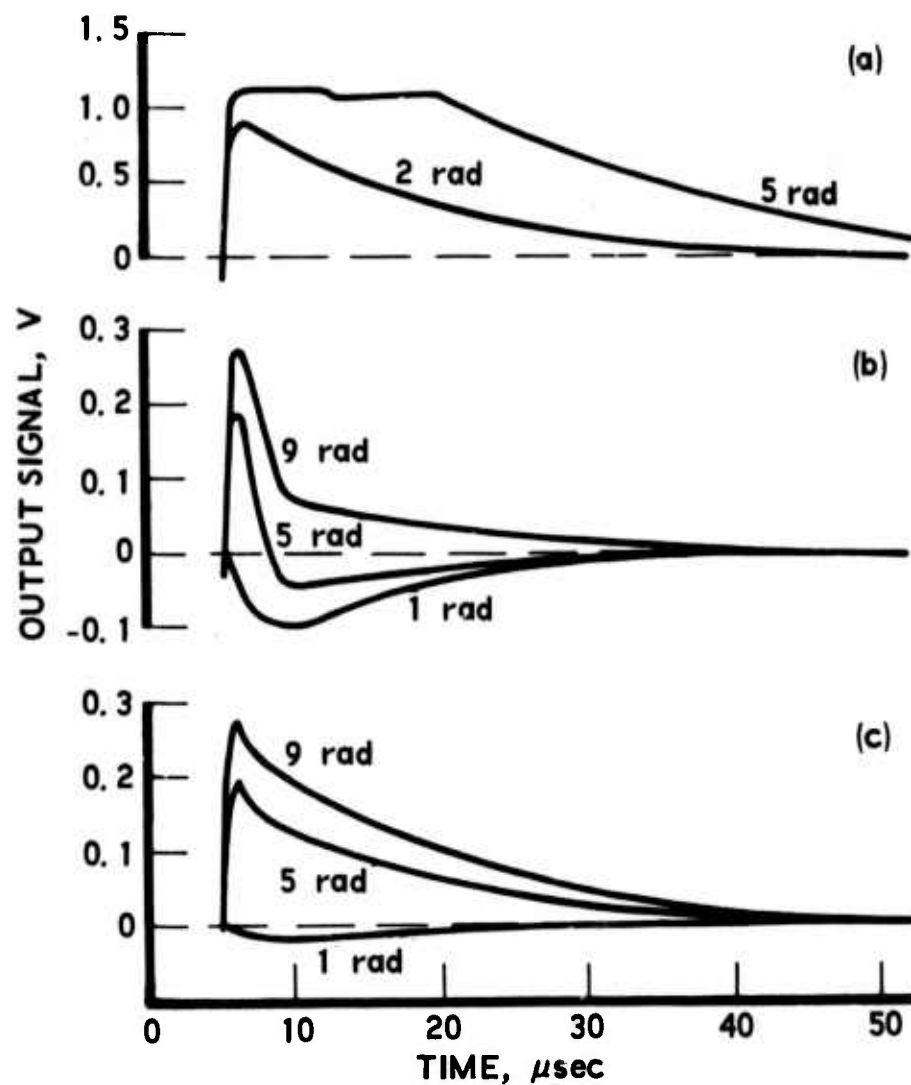


Fig. 9. Radiation Responses of $\mu A741$ Operational Amplifier Under Vacuum: (a) Total exposure of sealed unit, (b) Response of sealed unit with IC chip shadowed from x rays for three different doses, and (c) Response of open unit with IC chips shadowed from x rays for three different doses.

as that from photoemission off the external lead. Other DR testing was done with gains of 10 where $R_p = R_f$ or $R_p = R_i$. Results were very similar to the bench tests except that the signal polarities were reversed because the charge was induced by photoemission off the leads. During very intense shots with unbalanced input resistances, the output often showed complicated signals that first went negative and then positive and occasionally even negative again before decaying to zero. Final testing attempted to distinguish between TREE and IEMP effects by shadowing various parts of the operational amplifier with Pb. The perplexing observation was that the operational amplifier output was about the same when a Pb aperture was used so that only the IC chips were irradiated or a small Pb disc shadowed only the IC chips. On the other hand, the signals were different when the entire operational amplifier was exposed.

VI. DISCUSSION

Three typical IC operational amplifiers were irradiated by x radiation and by photoelectrons generated by a plasma focus discharge. Under most conditions, various portions of the operational amplifier output signals could be correlated with: (1) electron deposition on the output lead, (2) electron deposition on the external input leads, (3) electron emission or deposition of the input leads inside the operational amplifier housing, and (4) interaction of the photons with IC chips. The effects of electron deposition and photo-emission off the external leads were also studied in bench tests. Electron deposition on the output lead of an operational amplifier was observed as narrow negative transient pulses that matched the x-ray pulses; these were observed only during ED tests using a nearby Ta foil. Further confirmation of this effect was the appearance of these negative transients when the operational amplifier power supply was turned off.

Let us first analyze the magnitudes of the Q25 output signals resulting from electron deposition. Data from shots such as those shown in Fig. 5(a) showed that the amplifier output was reasonably proportional to the effective charge deposited on an input lead. We assume that the number of electrons deposited on each input and on the electron monitor are in the ratio of their areas. Then, the change q_{in} on an input is given by

$$q_{in} = \frac{V_{mon} \tau A_{in}}{50 A_{mon}} \quad (C)$$

where V_{mon} is the voltage observed across 50Ω on the monitor, $A_{mon} = 12 \text{ cm}^2$ is the monitor area, A_{in} is the collection area of the input wire, and τ is the observed width of the deposition signal (in this case equal to the 100-nsec integration time). The voltage induced on the input is $V_{in} = q_{in} / C_{in}$, and the calculated output voltage is $V_{out} = G V_{in}$. The input capacitances

were taken to be 6 and 7 pF. For the parameters $R_p = 0$, $R_i = 50 \text{ k}\Omega$, and $R_f = 500 \text{ k}\Omega$, where the gain was $G = 10$, only charge on the negative input had to be considered. The calculated output voltage agreed with the measured output to $\pm 25\%$ on each of six shots for an assumed area of $A_i = 0.30 \text{ cm}^2$. This area is consistent with the dimensions of the wires attached to the negative input. Similar good agreement was found for the five shots taken with $R_p = 200 \text{ k}\Omega$, $R_i = 5 \text{ k}\Omega$, and $R_f = 50 \text{ k}\Omega$ with $G = 11$. The calculated values then agreed with the measured values of the operational amplifier output to $\pm 30\%$ for an input area of $A_p = 0.18 \text{ cm}^2$, which corresponds to the lead dimensions of 0.07-cm diam and 2.5-cm length.

During direct irradiation tests of the operational amplifiers, the responses of the two relatively fast Q25 and 702 units were found to arise primarily from the deposition and emission of photoelectrons within the operational amplifier enclosures. But, the response of the slower 741 unit appeared to be largely from photon interactions (TREE) with the IC chip. The TREE responses, which were observed in the 702 and 741 units, produced positive output signals. On the other hand, the IEMP responses of the 702 and 741 units resulted in negative signals that corresponded to electron deposition on the positive lead. This can be explained by the negative potential of the housing relative to the grounded input leads so that low-energy electrons, particularly those created during gas ionization by primary photoelectrons, are driven to the grounded leads. The housing of the Q25 was grounded, and its responses corresponded to a net photoemission of electrons off the input leads. Oblique irradiation of the Q25 unit in the ED configuration showed that the photoemission from an input lead inside the housing had the same magnitude as electron deposition on the external lead from the surrounding Ta foils. Since we had only the single Q25 unit, we did not determine how much its IEMP response was enhanced by gas ionization effects.

Some of the observations when the tested operational amplifiers were driven into saturation are now discussed. As is well known, saturation

effects are usually very complicated to analyze. Bench tests showed that the $\mu A741$ responded differently for positive or negative charge injected on the noninverting input. For a large positive charge input, the 741 output remained in saturation for a time period proportional to the amount of charge injected on the noninverting input. Comparable amounts of pulsed negative charge injection did not drive the amplifier into saturation. This anomaly is at least partially attributed to the slow response of the amplifier circuit. During plasma focus irradiation tests on the 741, it seemed that the TREE responses dominated and the time duration in saturation was proportional to the x-ray dose inside the unit. This ratio of saturation time to dose was $30 \pm 7 \mu\text{sec}/\text{rad}(\text{Si})$ for a sealed or open unit in vacuum with doses of 1 to 3 rad(Si). This radiation response was the same whether R_p was 1 k Ω or 100 k Ω with $R_i = 1 \text{ k}\Omega$ and $R_f = 100 \text{ k}\Omega$. When units were irradiated with air or nitrogen in the chamber, the saturation times were decreased. This indicates that gas ionization enhanced the charge deposition on the external leads, thereby partially cancelling radiation responses of the unit.

The responses of the Q25 and 702 units were not simple when driven into saturation. As already noted, the outputs from the Q25 were different for positive charge on the input compared to negative charge input as shown in Fig. 3. When positive charge was injected on the positive input with $R_p \gg R_i$, the Q25 output was a simple positive signal in the linear regime and became complicated with the signal going first negative, then positive, and finally negative again for a large input. In other cases, the output first went negative and then remained in positive saturation. Such behavior can probably be explained by transistor saturation at different stages of the IC circuit and relevant RC time constants for charge to drain off at these stages. The responses of the $\mu A702$ unit had its own peculiar behavior characteristics in saturation. When sufficient negative charge was injected on the negative input, the operational amplifier output first went negative for a short time, then went positive for a duration that increased nonlinearly with input charge, and finally went into negative saturation for a while before dropping to zero. Radiation responses of other operational amplifiers will be studied in the future.